

# Reconstruction of reduced-order EHD flow fields using the proper orthogonal decomposition

Zelu Yan  
Logistics Engineering College  
Shanghai Maritime University  
Shanghai, China  
College of Information  
Science and Technology  
Donghua University  
Shanghai, China  
zlyan@shmtu.edu.cn

Christophe Louste  
PPRIME Institute  
CNRS-University of Poitiers-  
ENSMA  
Futuroscope-Chasseneuil,  
France  
christophe.louste@univ-  
poitiers.fr

Philippe Traoré  
PPRIME Institute  
CNRS-University of Poitiers-  
ENSMA  
Futuroscope-Chasseneuil,  
France  
philippe.traore@univ-  
poitiers.fr

Jian'an Fang  
College of Information  
Science and Technology  
Donghua University  
Shanghai, China  
jafang@dhu.edu.cn

**Abstract**—The proper orthogonal decomposition (POD) algorithm was applied to reconstruct the instantaneous velocity field of the EHD jet in this work. Particle image velocimetry (PIV) measurements were conducted on EHD jets in a blade-plane configuration at different voltages and electrode spacings. The acquired instantaneous flow fields were used as input to yield the orthogonal spatial modes, the temporal coefficients and the eigenvalues that are automatically ranked by kinetic energy magnitudes. It is shown that the dominant spatial modes obtained by POD usually correspond to large-scale coherent structures, while the higher modes characterize finer-scale turbulent vortex structures. Although POD-based flow field reconstruction allows for the elimination of non-coherent noise and spurious vectors in the original PIV data, the number of modes available for reconstructing the instantaneous flow field tends to increase due to the decrease in the energy content of the dominant modes.

**Keywords**—Proper Orthogonal Decomposition (POD); Particle Image Velocimetry (PIV); EHD flow; reconstruction

## I. INTRODUCTION

Uncovering the flow characteristics of electroconvection is the key to studying EHD pumping technology. Caused by the complex coupling of electric and flow fields, the essential physicochemical mechanism of EHD flows remains to be further investigated by the scientific community. One of the experimental methods that has proven its practicability so far is the particle image velocimetry (PIV), which plays an irreplaceable role in visualizing flow fields, building fundamental data sets, as well as validating theoretical analysis and simulation results. Given that the dielectric medium to which the tracer particles are added is subjected to a combined effect of electric and flow fields when using the PIV technique, several scholars have explored the effects of particle specification and concentration on the velocity field of EHD flows through theoretical and experimental studies [1,2]. It has been demonstrated that, with a reasonable choice, the seeding particles follow the fluid motion almost strictly, independent of other parameters of themselves [2]. Also before measurement, the time interval between two consecutive images should be pre-adjusted to minimize the number of uncorrelated vector fields [3].

However, although the above pre-processing techniques have greatly improved the quality of the PIV measurements, there are still many unpredictable spurious vectors with superimposed incoherent noises in an instantaneous flow field owing to turbulence and stability issues. The post-processing

of the system, which is actually more effective for the time-averaged flow field, appears to have no satisfactory solution to this problem. To effectively address the problem, this paper attempts to apply proper orthogonal decomposition (POD) analysis, which has become a common trend in fluid mechanics in recent years [4], to the field of electroconvection in dielectric liquids, with the aim of providing a method for PIV post-processing that can effectively remove non-coherent noise and spurious vectors from the instantaneous flow field of PIV data. In fact, this technique was previously reported in the analysis of plasma wake flow induced by a DBD actuator [5], and authors claimed that the reduced order model resulting from POD presents as an effective tool by which to analyze the coupled electric and hydrodynamic phenomena. In this work, we transfer POD to the dielectric liquid branch of the EHD for controlling these flows by means of the obtained spatial modes [4], in order to remove undesirable vectors by constructing reduced order flow fields, to gain insight into the flow physics and to identify the common structural features underneath various flow patterns.

The POD technique is a modal decomposition technique that was first introduced to the fluid dynamics and turbulence domain by Lumley [6]. It maps the original data set through a transformation and extracts a set of subspaces of a specific dimension consisting of a minimum number of basis functions or modes (reduced order modes) [7]. Thanks to the dominant spatial modes (lower order modes) obtained by POD demonstrating the coherent structure, the understanding of turbulence as the superimposition of a mean field on a randomly fluctuating velocity field has gradually shifted to that of a deterministic aspects of flows having a correlation structure [8]. Recently, scholars in the field of fluid mechanics have realized that flow features and phenomena that can be easily identified by simple visual inspection (e.g., von Kármán shedding, Kelvin-Helmholtz instability, and vortex pairing/merging) are necessary to be extracted by some mathematical procedures (e.g., POD analysis, dynamic mode decomposition (DMD), Koopman analysis, global linear stability analysis, resolvent analysis, etc.) [7]. This enables to reveal the dominant common structure of complex high-dimensional flows in low-dimensional modes, and thus to analyze these observations from their essence through phenomena. The above mentioned phenomena such as von Kármán shedding, vortex pairing and merging have been reported in EHD flows [9,10], so the application of modal analysis to the EHD field is very promising.

This work was supported by National Natural Science Foundation of China (Grant No. 51907118).

## II. METHODOLOGY

### A. Experimental procedure

All experiments were performed in a cubic cell in which a blade-plane actuator with adjustable electrode spacing was installed. The different voltage and electrode spacing result in the generation of various patterns of impinging jets. Since the experimental setup is the one used in the literature [3], only the key steps are briefly described in this paper. For more details, please refer to the above mentioned study. The physical properties of the dielectric liquid are as follows: mass density of 850 kg/m<sup>3</sup>, conductivity of 1.15×10<sup>-9</sup> S/m, relative permittivity of 2.2, and kinematic viscosity of 4.3 cSt. For each case, 1000 instantaneous fields were recorded as data sets for subsequent POD analysis.

In order to maximize the data quality of PIV measurements, tracer particles of SiO<sub>2</sub> with a concentration of 0.01 g/L and a diameter of 0.5 μm are added in our case. Furthermore, the different flow patterns corresponding to the various flow regimes of the EHD jets need to be visualized in pre-tests and a preliminary statistical analysis was carried out to guarantee the choice of the time interval Δt for later regular measurements. The pre-tests show that in our case, Δt=100 μs is usually valid for a moderate  $\bar{E}_{app}$ , ( $\bar{E}_{app}<15$  kV/cm, where  $\bar{E}_{app}$  is an apparent mean electric field equal to the ratio of voltage to electrode gap). Δt decreases with increasing  $\bar{E}_{app}$ , and Δt needs to be specified according to local conditions in higher electric field strengths.

### B. POD method

Since POD demands second-order spatial cross-correlation of velocities, the field-based PIV technique is naturally adapted to this approach [8]. In addition, POD is a purely objective data-driven algorithm, which has the advantage over other methods for large-scale structure identification. First, no *a priori* knowledge is required for deduction. Second, no input requirements are imposed, i.e., the set of data can be linear/nonlinear, numerical/experimental, and sequential/disordered. The POD of flow field data has three main methods, and their principles are roughly the same, so we only briefly introduce the implementation steps of classical POD here.

Upon obtaining the post-processing data of the PIV flow field, we are asked to remove the time-averaged velocity field from each instantaneous flow field of the original PIV data, so that we are left with only the flow field of the fluctuating components. Then, we are required to stack  $N$ -such two-dimensional flow field ( $p \times q$ ) data into a matrix  $X(N \times 2pq)$ , which is written as

$$X = \begin{bmatrix} u_{1,1}^1 u_{2,1}^1 \dots u_{p,1}^1 \dots u_{1,q}^1 u_{2,q}^1 \dots u_{p,q}^1 v_{1,1}^1 v_{2,1}^1 \dots v_{p,1}^1 \dots v_{1,q}^1 v_{2,q}^1 \dots v_{p,q}^1 \\ u_{1,1}^2 u_{2,1}^2 \dots u_{p,1}^2 \dots u_{1,q}^2 u_{2,q}^2 \dots u_{p,q}^2 v_{1,1}^2 v_{2,1}^2 \dots v_{p,1}^2 \dots v_{1,q}^2 v_{2,q}^2 \dots v_{p,q}^2 \\ \vdots \\ u_{1,1}^N u_{2,1}^N \dots u_{p,1}^N \dots u_{1,q}^N u_{2,q}^N \dots u_{p,q}^N v_{1,1}^N v_{2,1}^N \dots v_{p,1}^N \dots v_{1,q}^N v_{2,q}^N \dots v_{p,q}^N \end{bmatrix} \quad (1)$$

where an arbitrary element  $u_{m,n}^k$  (or  $v_{m,n}^k$ ) represents the horizontal (or vertical) fluctuating velocity component at the coordinates ( $m, n$ ) of the PIV flow field at instant  $k$ . In the matrix  $X$ , each row (representing the set of velocities at a given moment) starts with  $u$  (horizontal component) and ends with  $v$  (vertical component). It should be noted that since the

POD results are not affected by the way the matrix elements are arranged, there are no strict rules on how to stack the two-dimensional velocity field into one dimension (the row of  $X$ ). We simply need to make sure that stacking and unstacking is performed in a consistent manner. However, for the convenience of the subsequent analysis, we follow the original temporal and spatial order.

As mentioned earlier, the purpose of POD analysis is to find an optimal set of basis vectors (i.e., spatial modes). We seek the mapping approach that represents the original vectors with the least number of modes. The solution to this problem can be determined by finding the eigenvectors and eigenvalues of the covariance matrix of  $X$ .

$$R\phi_i = \lambda_i\phi_i \quad (2)$$

where  $R = X^T X / N$  is the covariance matrix representing the autocorrelation and cross-correlation between the values of all  $u$  and  $v$ . The eigenvector  $\phi_i$ , corresponding to the eigenvalue  $\lambda_i$  that characterizes the kinetic energy of the fluctuating flow field, is one of the POD modes. Note that POD modes are orthogonal (the inner product between modes is normal) [7]. The POD allows the eigenvalues to be ranked in decreasing order from largest to smallest, which guides us to focus attention on the lower order modes (when  $i$  is small). Similarly, all the fluctuating energy of the flow field is distributed into different modes, with the lower-order modes containing more flow field energy (characterized by eigenvalues). This enables a reduced-order flow field constructed by superimposing a limited number of modes to effectively reproduce the original flow field.

In order to reconstruct the original transient flow field, the POD temporal coefficient  $a_i$  is also required to depict the variation of each mode with time, the coefficient is given by

$$a_i(t) = X\phi_i \quad (3)$$

By summing the time-averaged flow field with the product of a finite number of independent temporal ( $a_i$ ) and spatial ( $\phi_i$ ) signals, we recover the original flow field to the maximum extent possible. The formula is in the form of

$$V \approx \bar{V} + \sum a_i(t)\phi_i \quad (4)$$

where  $V$  and  $\bar{V}$  are the instantaneous and time-averaged flow field, respectively, with the same matrix structure as  $X$ .

## III. RESULTS AND DISCUSSION

### A. Percentage of kinetic energy

Fig. 1 shows the fluctuating kinetic energy captured by each mode obtained by POD for the three cases. The kinetic energy contribution of each mode can be expressed as a percentage of the eigenvalues of the present mode to the sum of all eigenvalues. The rule that kinetic energy contribution decreases significantly with increasing modal order applies to all cases, which verifies the fact that the eigenvalues in the POD analysis are automatically ranked by energy magnitude. Specifically for each case, the energy contribution of the 1st-order mode reaches 38.2%, 23.8% and 4.6% for the low ( $\bar{E}_{app}=1.67$  kV/cm), moderate ( $\bar{E}_{app}=5$ kV/cm) and high ( $\bar{E}_{app}=13.3$  kV/cm) electric field, respectively. This result can be explained as follows. As the electric field  $\bar{E}_{app}$  increases, the EHD impinging jet experiences several regimes from intermittent charge injection to weak injection and then to strong injection [3], and the interaction between charge and

fluid progressively becomes stronger and more complex, which inevitably leads to a gradual increase in the number of physical structures that determine the flow field distribution. In other words, the stronger the electric field strength is, the greater number of modes characterizing the structural properties of the original flow field is demanded. Accordingly, the energy becoming more dispersed between modes results in a decrease in the energy proportion of the lower order modes.

By accumulating the energy percentage of each order of modes in Fig. 1, we obtain the cumulative energy contribution curves for the three cases in Fig. 2. It is clear that for low electric field strength ( $\bar{E}_{app}=1.67$  kV/cm), the number of modes needed to reach 63% and 90% of the total energy is 3 and 33, respectively, which indicates that the reduced-order reconstruction of the flow field can be achieved by storing only a small number of modes. The number of modes required increases for moderate electric field ( $\bar{E}_{app}=5$  kV/cm), i.e., 14 and 204. The case with the highest number of required modes (58 and 379) is under the strong electric field ( $\bar{E}_{app}=13.3$  kV/cm). The reason, as analyzed above, is that as the electric field increases, the lower-order modes are allocated increasingly smaller amounts of energy. The flow field reconstruction necessitates the involvement of more low-order modes. In addition, Fig. 2 also reflects that POD is a useful approach in storing and compressing large databases of EHD experiments.

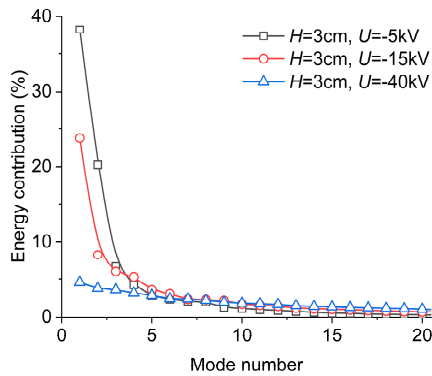


Fig. 1. Energy contribution of POD modes for three cases.

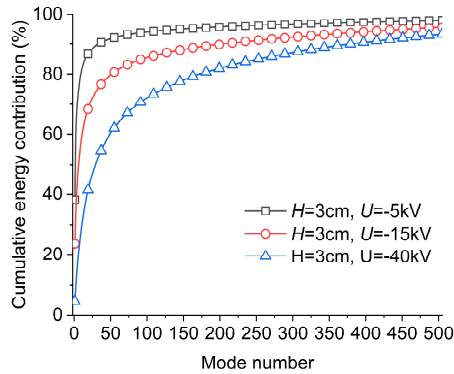


Fig. 2. Cumulative energy contribution of POD modes for three cases.

### B. Reconstruction of EHD flow field

Of the three cases in which the kinetic energy content of the modes was discussed in the previous section, we choose the case with the most severe condition for reconstruction, i.e.,  $H=3$  cm,  $U=-40$  kV, to demonstrate the reconstruction of the reduced-order flow field using POD. The lower-order and

higher-order modes of the POD, as well as the reconstruction of an instantaneous velocity field based on them are shown from Fig.3 to Fig.6. We can see that the instantaneous velocity field distribution, which is chaotic in turbulent flows, exhibits a well-ordered structure in the spatial modes of the POD, and these structures are mainly presented in the form of vortices through fluctuating velocities in our modes.

The main kinetic energy distribution of a flow can be effectively reflected by the first few orders of modes. It is evident that the kinetic energy of the EHD impinging jet induced by a strong electric field is mainly distributed in the middle and at the end of the centreline, while the energy at the initial and along-wall positions of the jet is hardly captured by the lower order modes (see Fig.3 and Fig.4). Instead, its smaller content of energy is found in higher order modes in finer scale turbulent vortex structure (see Fig.5). As the order of the mode increases, the number of vortices gradually increases, while the scale decreases.

In our case, the 2nd and 3rd -order modes (not shown in this paper) are very similar in structure and their energy content is comparable. The presence of two neighboring modes with similar structures in the lower order modes has also been observed in the POD modes of classical jets. The similar mode pairs were detected for the von Kármán vortex street observed in the cylindrical wake [11], as well as for the laminar separated flow on the flat plate wing [7] by the POD, and they were analyzed and found to be highly correlated with the coherent structures, which inspires us to perform a similar analysis for the EHD jet in the future.

Fig. 6 illustrates the comparison of the original flow field with the reconstructed flow field based on (4). We can use the eigenvalues to determine the number of modes needed (see Fig.2). In general, there is no strict rule on how many modes we keep to represent the flow. Based on the fact that the energy of our EHD jet is actually concentrated in the axis, we pick the first 73 orders of modes (representing 67% of the total energy) to reconstruct the flow field in this case. The results demonstrate that the low-order modes consisting of large-scale vortices dominate the flow structure of the jet. The main velocity distribution and the jet's profile remain nearly the same as those of the original jet. In addition, non-coherent noise introduced by small-scale turbulence (which contains little energy) in the ambient of the jet and spurious vectors (which have a low probability of being detected continuously) are assigned into higher-order modes without engaging in the reconstruction.

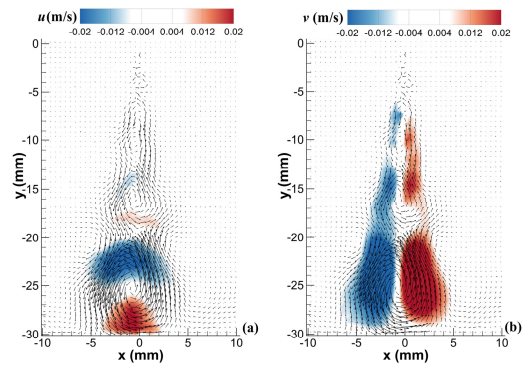


Fig. 3. The 1st-order mode associated with the captured fluctuation energy for the case  $H=3$  cm,  $U=-40$  kV. The vectors represent the fluctuating velocity field. The color map indicates the distribution of the horizontal fluctuating velocity  $u$  (a) and the vertical component  $v$  (b).

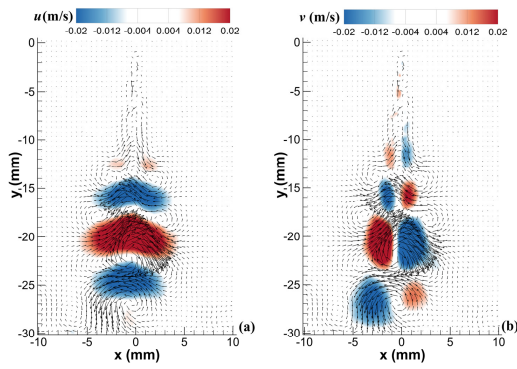


Fig. 4. The 2nd-order mode associated with the captured fluctuation energy for the case  $H=3$  cm,  $U=-40$  kV. The vectors represent the fluctuating velocity field. The color map indicates the distribution of the horizontal fluctuating velocity  $u$  (a) and the vertical component  $v$  (b).

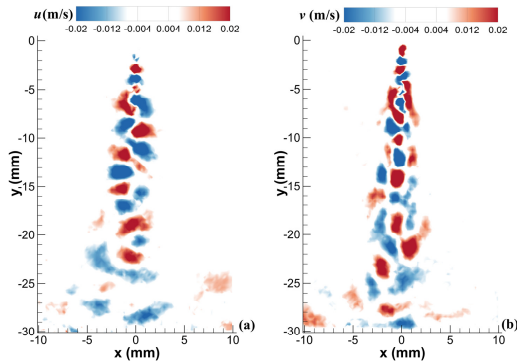


Fig. 5. The 69th-order mode associated with the captured fluctuation energy for the case  $H=3$  cm,  $U=-40$  kV. The color map indicates the distribution of the horizontal fluctuating velocity  $u$  (a) and the vertical component  $v$  (b).

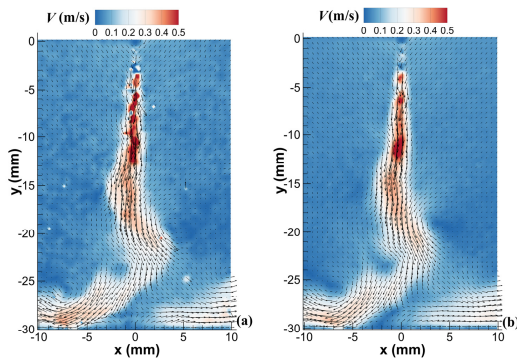


Fig. 6. Reconstruction of the instantaneous velocity field using the first 76 orders of POD modes for the initial moment ( the first measured velocity field with  $k=1$ ). The vectors represent the velocity field. The color map denotes the modulus of the instantaneous velocity. The original PIV flow field (a) and the reconstructed flow field (b) are shown for comparison.

## CONCLUSIONS

In this paper, the POD method was employed to obtain a set of orthogonal basis vectors with minimum dimension from the original PIV velocity field, and these so-called spatial modes were used to construct the reduced-order flow fields. The eigenvalues characterizing the amount of energy contained in modes can guide us to select a finite number of modes to recovery the instantaneous flow field. The results show that small-scale noise as well as spurious vectors can be effectively removed after the exclusion of higher-order modes, and the main jet is well preserved for subsequent analysis. This provides a reference for the post-processing technique of PIV in the field of EHD experiments. Besides, the physical mechanism that dominates the complex flow of EHD jets can be revealed in low-order modes, where we observe clearly the large-scale vortices distributed in the streamwise direction near the jet axis. For future work, we will focus on the spatio-temporal correlation of low-order mode pairs to interpret the coherent structure.

## REFERENCES

- [1] M. Daaboul, C. Louste, and H. Romat, "PIV Measurements on Charged Plumes-Influence of  $\text{SiO}_2$  Seeding Particles on the Electrical Behavior," *IEEE Trans. Dielectr. Electr. Insul.*, vol. 16, no. 2, 2009.
- [2] C. Gouriou, P. Traoré, and C. Louste, "Influence of Seeding Particle Type on Velocity Measurements in Silicone Oil Under High Voltage," *IEEE Trans. Ind. Appl.*, vol. 53, no. 3, pp. 2471-2476, 2017.
- [3] Z. Yan *et al.*, "Structural characteristics of electrohydrodynamic jets induced by a blade-plane actuator subjected to highly non-uniform electric fields: Parametric investigation through the particle image velocimetry techniques," *High Voltage*, 2022.
- [4] C. W. Rowley and S. T. M. Dawson, "Model Reduction for Flow Analysis and Control," *Annual Review of Fluid Mechanics*, vol. 49, no. 1, pp. 387-417, 2017.
- [5] D. A. Juan *et al.*, "Reduced order models for EHD controlled wake flow," *Journal of Physics: Conference Series*, vol. 166, no. 1, p. 012014, 2009.
- [6] J. L. Lumley, "The Structure of Inhomogeneous Turbulence," *Atmospheric Turbulence and Wave Propagation*, 1967, pp. 166-178.
- [7] K. Taira *et al.*, "Modal Analysis of Fluid Flows: An Overview," *AIAA Journal*, vol. 55, no. 12, pp. 4013-4041, 2017.
- [8] Y. M. Shim, R. N. Sharma, and P. J. Richards, "Proper orthogonal decomposition analysis of the flow field in a plane jet," *EXP THERM FLUID SCI*, vol. 51, pp. 37-55, 2013.
- [9] P. Traoré *et al.*, "Electrohydrodynamic Plumes due to Autonomous and Nonautonomous Charge Injection by a Sharp Blade Electrode in a Dielectric Liquid," *IEEE Trans. Ind. Appl.*, vol. 51, no. 3, pp. 2504-2512, 2015.
- [10] Z. Yan, C. Louste, and J. Wu, "Characteristics of an Electrohydrodynamic Jet Induced by Electrochemical Injection and Field-Enhanced Dissociation in a Blade-Plane Geometry," *IEEE Trans. Dielectr. Electr. Insul.*, 2022.
- [11] K. Taira *et al.*, "Modal Analysis of Fluid Flows: Applications and Outlook," *AIAA Journal*, vol. 58, no. 3, pp. 998-1022, 2019.